

# Wind Driven SM-BDFIG for Remote Areas in Egypt

Mahmoud A. Saleh, Maged N. F. Nashed, Mona N. Eskander

Electronics Research Institute, Cairo, Egypt

mahmoudsaleh36@yahoo.com, maged@eri.sci.eg, eskander@eri.sci.eg

**Abstract :** *In this paper an integrated system of WECS, battery storage and controller is proposed to supply electrical energy to a small community in a remote area in Egypt. The layout and the configuration are presented and discussed. Also, a new wind speed frequency distribution model is proposed based on the prevailing wind speed in this area. The validity of the model is tested for different sites in Egypt. The model and the relevant equation express the wind speed frequency distribution in terms of the prevailing wind speed in the site and its frequency distribution, hence it can be applied for any site all-over the world with known wind speed profile. Based on this model, the size and rated speed of the WECS to provide electrical energy to the specified loads in this remote area can be determined.*

**Keywords :** WECS, DFIG, Bi-directional converter, and Micro-grid.

## I. Introduction

Wind energy is now playing a key role in supplying competitive, reliable, and clean energy to support economic growth and to eliminate air polluting emissions. The average cost of wind energy reached 37cents/kWh compared to 61cents/kWh of the combined cycle gas fuelled power plants [i]. Large installed wind farms are usually connected to national or local grids.

In this paper, the authors propose utilizing wind energy conversion systems (WECS) to provide electrical energy in Egypt's remote areas having reasonable wind potential. The proposed system can be applied to remote areas in any country as it is applicable in Egypt. Egypt's area is about one million square kilometres, and the 90 million Egyptian population live on less than 5% of this area. The 95% remaining area is mostly deserts where small scattered communities (tribes, bedouins,..etc.) are living where underground water is available. The remote areas are defined by the well known 3-D definition, namely; **D**istance from urban areas, and consequently from national grid is large; **D**ensity of population is low; and **D**evelopment rate is lower than in urban areas. Mostly they use diesel –generator sets for electric power supply. The electrical loads for such communities can be classified in three categories: *i)* Essential loads such as hospitals, police stations, etc. for which the electrical power supply must be ensured all the time. *ii)* Normal loads such as households, small and medium industries, commercial activities ...etc. for which the electrical power supply is needed for several hours and can tolerate the supply cut-off for some time. *iii)* Flexible load such as water pumping, water desalination, ..etc., which can be supplied by electrical power when there is excess power due to higher wind power or longer periods of high wind speeds. Water for these flexible loads can be stored in water tanks to be utilized as required.

The single-machine brushless double-fed induction generator (SM-BDFIG) is the type of generator [ii] most suitable for WECS installed in such remote areas, since it can be operated without connection to an electrical grid and it does not need frequent maintenance due to the absence of brushes, together with the other known merits of the DFIG.

In the first section of this paper the layout of the proposed system and the configuration of the WECS, the storage battery bank, the controller, and the loads are presented and discussed. In the second section of the paper the wind characteristics of the chosen site are investigated and a new simplified model for the wind speed frequency distribution is proposed and verified using the annual and monthly wind data of six sites in Egypt. Three of these sites are on the Red sea coast and three on the Mediterranean coast. The wind data at two of these sites are given at two different heights, 10 and 20 meters. The proposed and verified simple model for predicting the wind speed frequency distribution can be applied for any site in any country. This model is based on the prevailing wind speed and its frequency rather than the average wind speed as in the previously well known models [iii]. Using the proposed model and the power-speed curve of the wind turbine, the generated electrical energy can be estimated for turbines with different rated speeds. Thereafter, the most adequate WECS for the site can be selected.

## II. The Proposed System Components

The proposed stand-alone WECS, shown in Fig.(1), consists of a wind turbine electrically coupled to a bi-directional converter, a battery bank, PLC for controlling the system operation, and three types of loads; an essential load, normal load, and a flexible load.

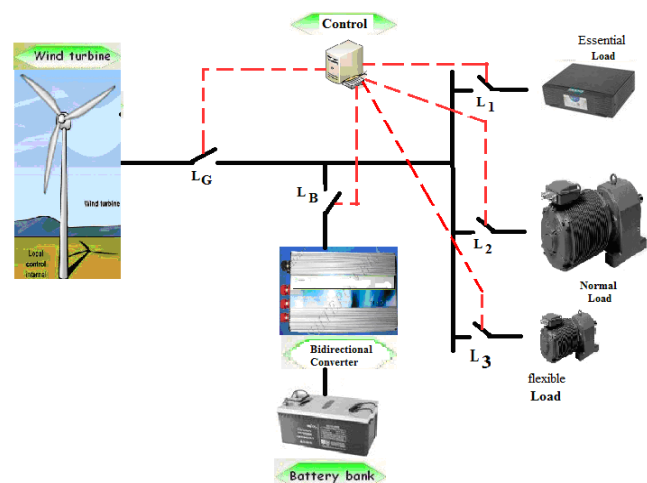


Figure 1, Layout of the proposed system.

The novel design of the SM-BDFIG was proposed by the first author of this paper, [ii]. The bi-directional converter either charges the battery bank when the available wind energy exceeds the load demand, or supplies the load demand from the battery bank when wind energy is less than the essential load demand. The PLC controls the switches to manage the system operation as shown in Table (1).

Table 1: modes of Operation

Wind Speed	State of Switches				
	Battery $L_B$	Generator $L_G$	Essential Load $L_1$	Normal Load $L_2$	flexible Load $L_3$
$0 \leq W < W_c$ or $W \geq W_o$ $I_B = I_{Bn}$	Close	Open	Close	Close	Open
$0 \leq W < W_c$ or $W \geq W_o$ $I_B < I_{Bn}$	Close	Open	Close	Open	Open
$W_c \leq W < W_r$ $I_G < \gamma I_{Gn}$	Open	Close	Close	Open	Open
$W_c \leq W < W_r$ $I_G \leq I_{Gn}$ $V_B < V_{Bch}$	Close	Close	Close	Close	Open
$W_r \leq W < W_o$ $I_G = I_{Gn}$ $V_B < V_{Bch}$	Close	Close	Close	Close	Close
$W_r \leq W < W_o$ $I_G = I_{Gn}$ $V_B \geq V_{Bch}$	Open	Close	Close	Close	Close

### 1. The SM-BDFIG

SM-BDFIG, as proposed by the first author [ii], is composed of three main components; a regular three phase wound rotor induction machine, a power electronic converter, and a pack of rechargeable Lithium-ion batteries. The converter is mounted on the outer surface of a web reinforced hollow metallic (aluminum) or fiber glass cylinder. The battery packs are embedded in the inner part of the cylinder between the webs. The hollow cylinder is mechanically coupled with the induction machine on the same shaft. Therefore, all the three main components of the SM-BDFIG rotate with the same angular speed.

### 2. The Bi-Directional Converter

The adopted converter, shown in Fig. (2), achieves ac/dc bidirectional conversion to charge the battery bank when surplus wind power is available, and to supply the essential load demand during low wind power intervals, [iv].

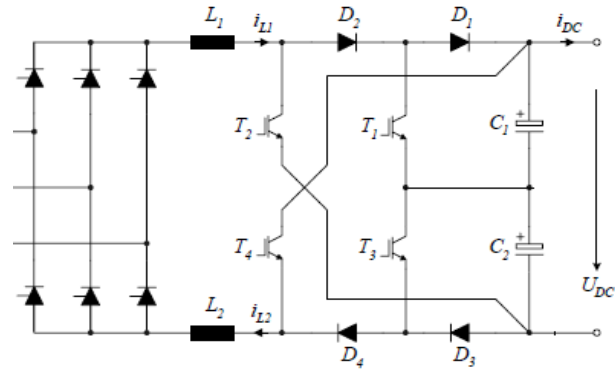


Figure 2, Bi-directional AC-DC converter with sinusoidal currents.

### 3. The Battery Bank

Lithium ion (Li-ion) battery bank is adopted in the proposed WECS due to its known merits. Several models for the LI-ion battery were adopted in the literature, e.g. the internal resistance model (IR), the one-time constant model (OTC) and the two-time constant model (TTC). Modelling is used to determine the state of charge (SOC) of the battery bank in order to determine the mode of operation of the proposed WECS. The TTC model, shown in Fig. (3), is composed of four parts voltage source VOC, ohmic resistance  $R_o$ ,  $R_{TTC1}$  and  $C_{TTC1}$  to describe the short term characteristics,  $R_{TTC2}$  and  $C_{TTC2}$  to describe the long term characteristics.  $v_{TTC1}$  and  $v_{TTC2}$  are the voltages across  $C_{TTC1}$  and  $C_{TTC2}$  respectively.  $i_{TTC1}$  and  $i_{TTC2}$  are the outflow currents of  $C_{TTC1}$  and  $C_{TTC2}$  respectively, [v].

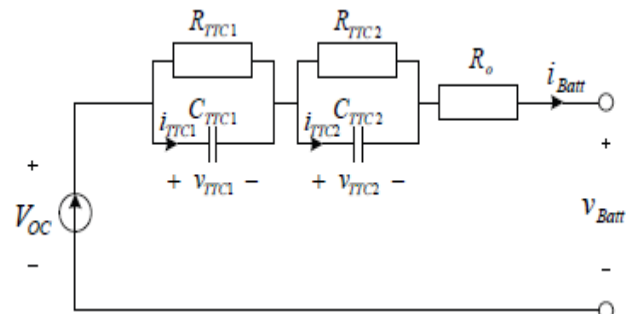


Figure 3. Battery equivalent circuit.

### III. System Modes of Operation

Referring to Table (1), the first mode of operation takes place when the wind speed  $W$  is lower than the cut-in speed  $W_c$  and the battery is fully charged. Hence the battery bank supplies the essential load and the normal load via closing switches  $L_B$ ,  $L_1$ , and  $L_2$ . The same switching mode applies when  $W$  is higher than the cut out speed  $W_o$  and the battery is fully charged.

The second mode of operation takes place when the wind speed  $W$  is lower than the cut-in speed  $W_c$  and the battery is not fully charged. Hence the battery bank supplies the essential load only via closing switches  $L_B$ ,  $L_2$  while the other switches are opened. The same switching mode applies when  $W$  is higher than the cut out speed  $W_o$  and the battery is not fully charged.

The third mode of operation takes place when the wind speed  $W$  lies between the cut-in speed and the rated speed  $W_r$  while the

generator current is lower than the load demand and the battery current is low. Hence the SM\_BDFIG supplies the essential load only via closing switches  $L_B$  and  $L_1$ .

The fourth mode of operation takes place when the wind speed  $W$  lies between the cut-in speed and the rated speed  $W_r$  while the generator current equals the load demand. Hence all loads are supplied by the generator via closing switches  $L_g$ ,  $L_1$ , and  $L_2$ .

The fifth mode of operation takes place when the wind speed  $W$  lies between the rated speed and the cut-out speed  $W_o$  while the generator current exceeds the load demand. The generator supplies the three types of loads and charges the batter bank, thus all switches are closed.

The sixth mode of operation takes place when the wind speed  $W$  lies between the rated speed and the cut-out speed  $W_o$ , the generator current exceeds the load demand and the battery is fully charged. The generator supplies the three types of loads and switch  $L_B$  connecting the battery bank is opened.

#### IV. Wind Speed frequency distribution Modeling and WECS Sizing

Wind data for six sites in Egypt [vi] are analyzed. The selected sites are Ras Ghareb (28.351° N, 33.08° E), Hurgada (27.258° N, 33.812° E), and Ras Shokeir (28.136° N, 33.277° E) on the Red Sea coast; Ras El Hekma (31.218° N, 27.851° E), El Obayed (31.386° N, 27.065° E), and El Kasr (31.37° N, 27.159° E) on the Mediterranean Sea coast. The available data is at 10 m and 20 meter height. The data was in the form of annual and monthly wind speed frequency distribution versus hours and time percentage for one meter/sec wind speed intervals. Since the amount of data is huge, only a sample of annual and one-month data are shown in table (2).

Table (2) the actual data of wind speed in Ras Ghareb 10m

Wind Speed (m/s)	Aug			Annual Summary		
	No. of hr	% of time	$f/f_p$	No. of hr	% of time	$f/f_p$
0	0	0	0	0	0	0
1	0	0	0	10	0.1	0.008
2	0	0	0	126	1.5	0.126
3	0	0	0	345	4.0	0.336
4	0	0	0	512	5.9	0.496
5	9	1.27	0.068	516	6.6	0.504
6	23	3.26	0.174	620	7.2	0.605
7	35	4.96	0.265	787	9.1	0.765
8	82	11.61	0.621	908	10.5	0.882
9	121	17.14	0.917	1031	11.9	1
10	132	18.7	1	1023	11.8	0.992
11	122	17.28	0.924	1009	11.7	0.983
12	82	11.61	0.621	824	9.5	0.798
13	43	6.09	0.326	556	6.4	0.538
14	38	5.38	0.288	259	3.0	0.24
15	19	2.69	0.144	89	1.0	0.08
16	0	0	0	16	0.2	0.016
17	0	0	0	3	0.0003	0.0029
18	0	0	0	0	0	0

The following analysis is carried out for the annual wind speed frequency distribution as function of the relative wind speed  $x$ , where  $x=W/W_p$ ,  $W$  is the wind speed and  $W_p$  is the prevailing wind speed, i.e. the speed with highest frequency occurrence. Statistical analysis of the available data together with mathematical manipulations proved that the general shape of the wind speed frequency distribution  $f$  can be expressed as:

$$\frac{f}{f_p} = \exp\left(\frac{1}{n}\right) \cdot x \exp\left(-\frac{x^n}{n}\right) \quad (1)$$

where

$n$  is an integer of 3,4,5,6,..etc.

$f_p$  the prevailing wind speed frequency

Comparing these sets of curves, shown in Figure (4), with the actual measured annual data for the six sites, the value of  $n=4$  seems to reflect the nearest model for the wind speed frequency distribution curves when compared to the actual data.

Hence , 
$$\frac{f}{f_p} = 1.284 \cdot x \exp\left(-\frac{x^4}{4}\right) \quad (2)$$

is adopted as the standard model. This model is compared with the data of Red sea as shown in Fig. 5 a, b and c, and the data of Mediterranean coast as shown in Fig. 6 a, b and c.

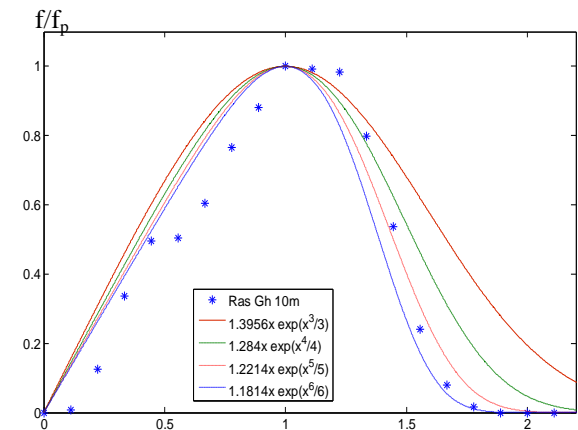


Fig. 4, Different alternatives of the model ( $n= 3,4,5$  and 6) compared to actual data of Ras Ghareb.

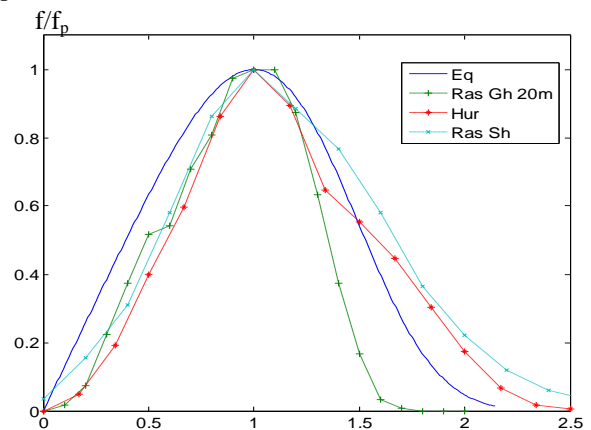


Fig. 5a, The annual data of Red sea and the model equation.

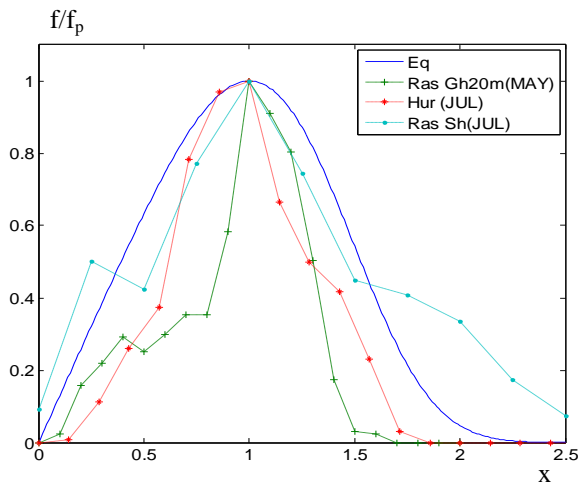


Fig. 5b, The month of highest wind speed and the model of Red sea.

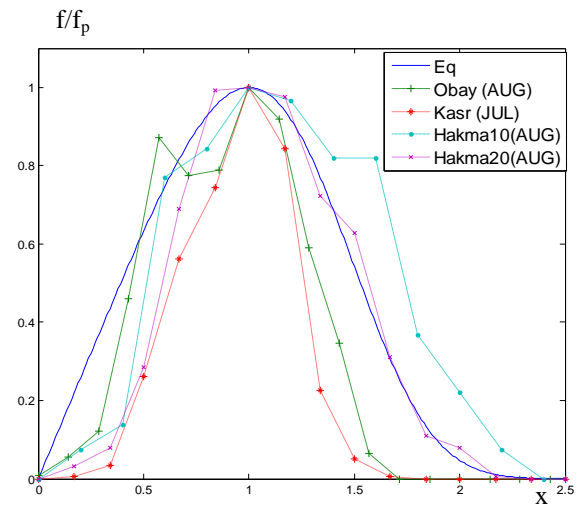


Fig. 6b, The month of highest wind speed and the model of Mediterranean coast.

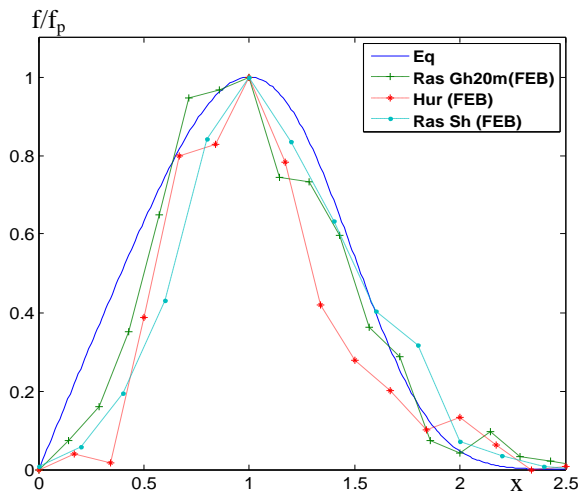


Fig. 5c, The month of lowest wind speed and the model of Red sea.

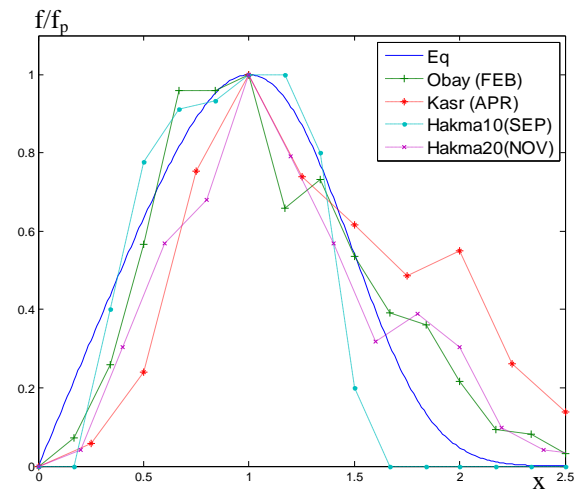


Fig. 6c, The month of lowest wind speed and the model of Mediterranean coast.

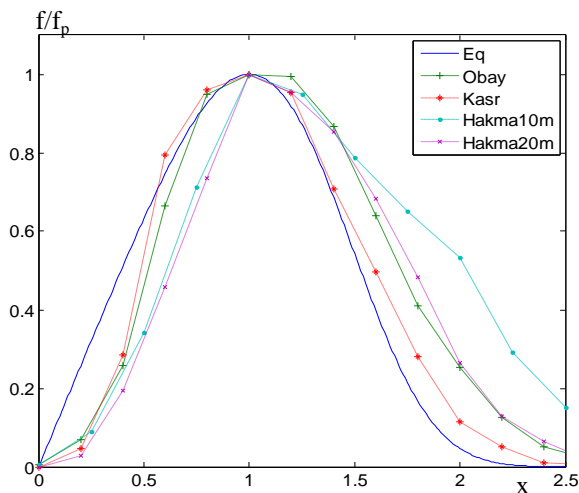


Fig. 6a, The annual data of Mediterranean coast and the model equation.

The model given by equation (2) will be adopted as the standard wind speed frequency distribution curves for sites in Egypt (since the authors have no access to wind data for other countries). The authors expect that the above concluded wind frequency distribution expression will be tested and its validity proven by wind experts in countries other than Egypt.

The wind power converted to mechanical power by the wind turbine at any wind speed  $W$  (or relative speed  $x$ ) is represented by the wind power curve shown in Fig. (7), and expressed as:

$$P = P_r \cdot (x^2/x_r^2) \quad \text{for } x_r > x \quad (3)$$

$$\text{And } P = P_r \quad \text{for } x \geq x_r \quad (4)$$

Where

$P$  = the power at wind speed  $W$  (relative speed  $x$ )

$P_r$  = rated output power of the wind turbine

$x$  is the relative speed ( $W/W_p$ )

$x_p$  is the relative rated speed ( $W_r/W_p$ )

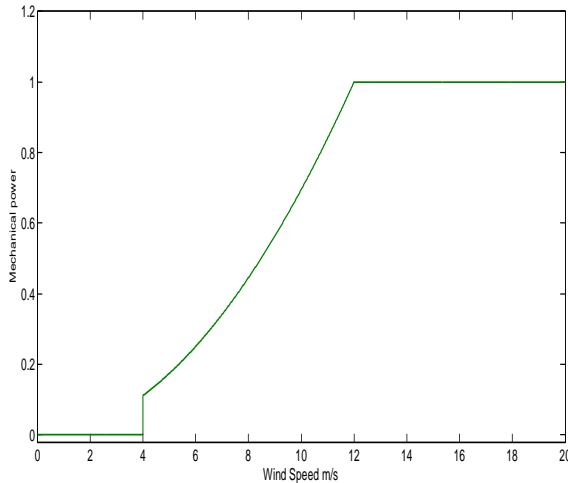


Fig. 7, The mechanical power versus the wind speed.

The energy generated for a period of time "f.T", where T is the total number of hours per year, is:

$$dE = P \cdot f \cdot T \cdot dx \quad (5)$$

The annual amount of wind energy converted to mechanical energy is:

$$E = \int_{x_c}^{x_o} P \cdot f \cdot T \cdot dx \quad (6)$$

From equations b, c, d, e, and f the following expression for the total energy is given as:

$$E = 1.284 P_r T \left[ \int_{x_c}^{x_r} \frac{x^3}{2} \exp\left(-\frac{x^4}{4}\right) dx + \int_{x_r}^{x_o} x \exp\left(-\frac{x^4}{4}\right) dx \right] \quad (7)$$

$$E = P_r \cdot T \cdot f_p \cdot I \quad (8)$$

Where

$x_c$ ,  $x_r$ , and  $x_o$  are the relative cut-in, rated, and cut-out speed respectively.

$W_c$ ,  $W_r$ , and  $W_o$  are the actual cut-in, rated, and cut-out speed respectively.

$$I = 1.284 \left[ \int_{x_c}^{x_r} \frac{x^3}{2} \exp\left(-\frac{x^4}{4}\right) dx + \int_{x_r}^{x_o} x \exp\left(-\frac{x^4}{4}\right) dx \right] \quad (9)$$

The integral I is calculated numerically for different values of  $X_r$  ( $0.8 \leq x_r \leq 1.2$ ) and for two sets of value, namely ( $X_c = 0.3$ ,  $X_o = 2$ ) and ( $x_c = 0.3$ ,  $x_o = 3$ ). Also the total annual amount of energy converted by the wind turbine may be expressed as:

$$E = P_r C_f T \quad (10)$$

Where

$C_f$  is the capacity factor of the wind turbine at this specific site

From equations (8) and (10) the capacity factor  $C_f$  can be expressed as:

$$C_f = f_p I \quad (11)$$

Hence by knowing the prevailing wind speed and its frequency for a given site, different alternatives of wind turbines to match

the electrical load demand for the given remote community can be chosen provided that  $P_r \geq (P_L + P_e)$

Where

$P_L$  is the peak of the regular load of this community

$P_e$  = the essential load of the community

Also,

$$P_r C_f = (C_L P_L + P_e)$$

i.e.  $P_r$  should be slightly larger ....

$$P_r \geq (C_L P_L + P_e) / C_f \quad (12)$$

$C_L$  = annual load factor of the remote community regular load (average of the load curve across the whole year)

The integral I versus the relative rated wind speed  $x_r$  for two values of cut-out speed ( $x_r = 2$  and 3) are shown in Fig. (8).

The capacity factor for a wind turbine with known rated speed  $x_r$  and cut-off speed  $x_o$  erected in any site in Egypt with available prevailing wind speed frequency distribution can be easily determined from Fig. 8 (-integral curve) and equation 10. The cut-off speed of most commercial WECS lies between two to three times the rated speeds. Hence sizing the turbine can be done for any site.

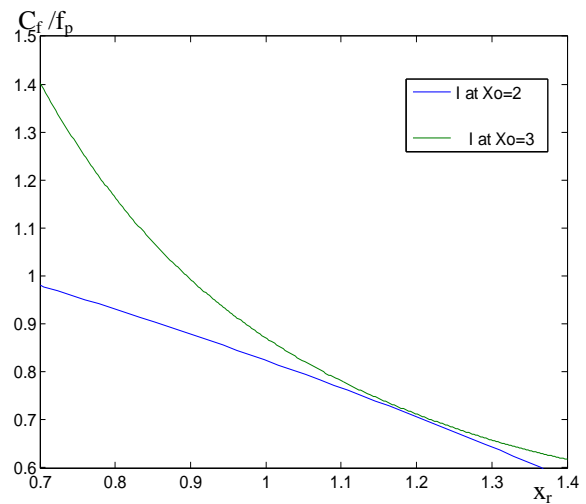


Fig. 8, I ( $C_f/f_p$ ) versus relative rated wind speed.

## V. Conclusion

Wind energy is expected to play an important role in providing electric power supply to the small communities in some remote areas of Egypt. Therefore, a micro-grid with its main components (WECS, storage battery, converter and controller) is proposed and briefly investigated in the paper as a step towards more developments in this area. The generator associated with the WECS is proposed to be SM-BDFIG since it is more adequate to remote areas than any other known type of the generators.

A novel equation for the wind speed distribution is proposed based on the prevailing speed in the site. The derived novel equation is tested for six sites in Egypt. It can be also applied in any site where the prevailing wind speed frequency is known. Applying this equation allows sizing of the wind turbine to be installed in a given site. Hence, economy is achieved when the

correct size of the turbine is known preventing over-sizing or de-sizing of the turbines, which adversely affects supplying the required loads.

## References

i. *Wind and Solar Energy* by Guest Editorial, *IEEE Power and Energy Magazine*, Nov-Dec 2015.

ii. Mahmoud A. Saleh and Mona N. Eskander, "A Single Machine Brushless DFIG for Grid-Connected and Stand-Alone WECS" *British Journal of Applied Science & Technology*, Vol.4, No.24, July 2014.

iii. D.Weisser, "A Wind Energy Analysis for Grenada: an estimation using the Weibull density function", *Renewable Energy*, Vol 28, No 11, 2003, pp 1803-1813.

iv. Maged. N. F. Nashed and Iman Edwar, "Wind/PV Hybrid of DC Electric Vehicle Charging Station with Bi-directional Converter" *World Engineering conference and Convention (WEEC 2015)*, Kyoto, Japan, 29 Nov. -2 Dec., 2015.

v. Ari Hentunen, Teemu Lehmuspelto, and Jussi Suomela, "Time-Domain Parameter Extraction Method for Th'evenin-Equivalent Circuit Battery Models", *IEEE Trans. on Energy Conversion*, Vol. 29, No. 3, September 2014, pp. 558-566.

vi. Mahmoud A Saleh, "Report on Mission to Egypt", UNESCWA,E/ESCWA/NR/87/6,23 March 1987